

LOAD RESPONSE AND FAILURE OF THICK RTM COMPOSITE LUGS

Markus Wallin¹, Olli Saarela¹ and Francesco Pentto²
¹Helsinki University of Technology and ²Patria Finavicom

Keywords: *composite lug, RTM, load response*

Abstract

Load response and failure of a thick composite lug was studied analytically and experimentally. The objective of the study was to get information on the stiffness, strength and failure mode of the lug, as well as on the applicability of the analysis method used to predict lug load response and failure.

The analyses were performed using finite element method. Parabolic solid brick elements were used. A steel pin was modeled to apply the loading. The loading was applied with a constant force distribution through the center of the pin. A contact was defined between the pin and the surrounding lug surface.

The test lugs were manufactured with the Resin Transfer Molding (RTM) technique. The outer and inner diameters of the lug were 145 and 75 mm, respectively. The ratio of the diameters was thus 1.93, which can be considered as a very small value for a composite lug.

The test specimens were loaded parallel to the lug centerline and in a 27° angle to the centerline. Five specimens were tested. Two of them were instrumented with 6 strain gages.

The measured strains showed fairly good correlation with the analysis results. The strain response was almost linear. However, the measured failure loads were significantly higher than the predicted ones. Still, it can be concluded that with correct material properties the FE approach used in the analyses can provide a reasonable estimate for the load response and failure of thick composite lugs.

1 Introduction

The use of Resin Transfer Molding (RTM) technique in aerospace composite manufacture enables higher level of part integration than conventional technologies. Natural parts to be integrated with the structure are attachment and actuator lugs e.g. in control surfaces of an aircraft.

For metallic lugs design guidelines are available (e.g. in [1]). However, these can not be directly used in composite lugs. The anisotropic nature of composites changes structural behavior significantly when compared to metallic lugs.

When a solid laminate is used and the lug shape is machined, the problem arises when the edge distance becomes small. The fibers in critical cross-sections are cut short and may not be able to carry loads as efficiently as in a continuous laminate. The matrix may not be able to transfer loads between fibers and the failure is dominated by shear. As a result the load carrying capability of the lug may be considerably low compared to the predictions obtained with traditional laminate analysis techniques.

A feasibility program was launched to study load response and load carrying capability of thick composite lugs [2].

2 Background

The RTM composite lug under investigation was designed to be used in control surfaces of a civil aircraft. Therefore, the space available for the lug was limited and the only way to increase

load carrying capability of the lug was to increase its thickness. With the applied pin and bearing, the end result was a thick lug with small edge distance.

2.1 Geometry

The length of the lug was 347.5 mm and the width 145 mm. The nominal thickness was 39.2 mm. The dimensions of the lug are presented in Fig. 1. The four holes ($\text{Ø}16$ mm) were used to attach steel plates of the test fixture to the specimen.

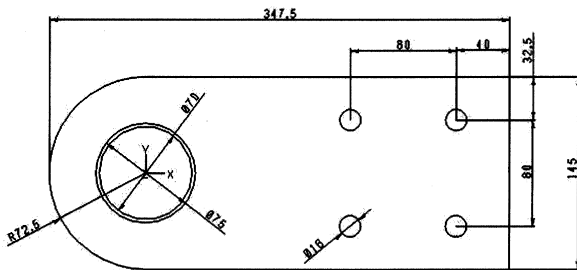


Fig. 1. Dimensions of the RTM lug.

2.2 Materials and Laminate Structure

The materials used in the lug were Hexcel G986 bindered twill fabric and RTM6 epoxy resin. Both materials are qualified for aerospace use. The laminate structure consisted of two sublaminates:

Laminate 1: $[0/45/45/45/0]_{SO}$, 9 plies

Laminate 2: $[0/45/0/45/0]_{SO}$, 9 plies

The final laminate structure of the lug was: [Laminate 1/11×Laminate 2/Laminate 1]. The total number of plies was 117.

A sliding bearing (Glacier MB7040DU) was used in the lug to prevent direct contact of the steel pin with the composite structure.

2.3 Load Cases

The lug was loaded in two ways: parallel to the lug centerline and in 27° angle to the lug centerline. The load cases are illustrated in Fig. 2.

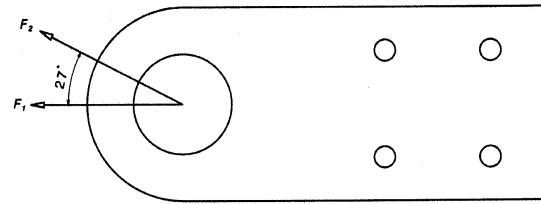


Fig. 2. Lug load cases.

3 Lug Analyses

An engineering type approach was selected for lug analyses. The problem was solved using finite element method (FEM). The model size was relatively coarse to keep the solving time reasonable. The software used in FE-analyses was I-DEAS [3] and in laminate analyses ESAComp [4]. The failure load analysis was based on the Tsai-Hill criterion.

The analysis type used was linear static analysis with contact definition resulting to an iterative solution. Linear material behavior and small displacements were assumed.

3.1 Modeling

The material in structural analyses was assumed to be homogeneous and orthotropic. The FE-model of the lug consisted of 3008 solid parabolic brick elements. The pin was modeled using 1280 parabolic solid elements consisting of both brick and wedge elements. A contact was defined around the pin. The bolts in the attachment points were modeled using beam elements. The 27° angle load case was arranged by rotating the specimen. The steel plates of the test fixture were modeled using rigid elements. The force was applied in the center of the pin as a constant force distribution through the thickness. The load used in the analyses was 100 kN. The FE-models used in the analyses are presented in Fig. 3. The solving time of one load case on a SGI Indigo2 R10000 workstation was approximately 3 hours.

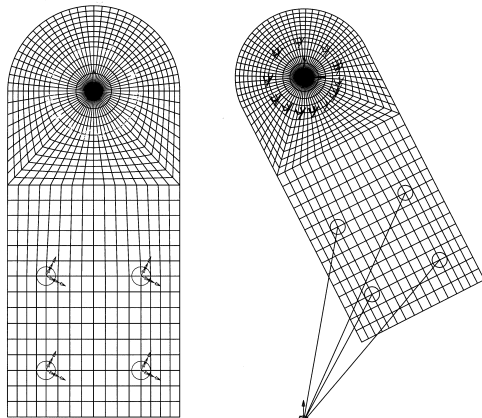


Fig. 3. Finite element models of the lug.

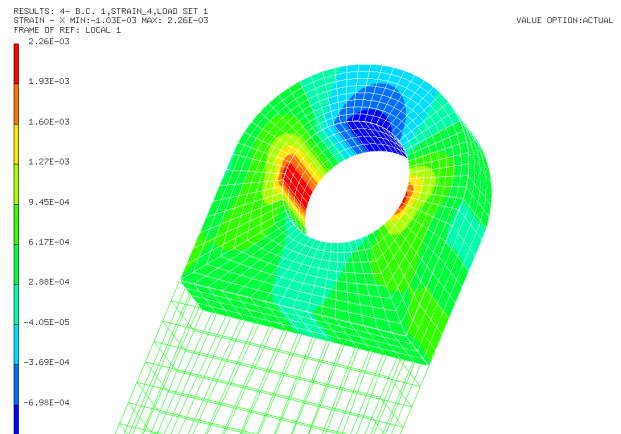


Fig. 4. Normal strains in straight tension, $F = 100$ kN.

3.2 Material Properties

Ply properties used in the analyses are presented in Table 1. The material properties are a combination of estimated and previously measured values for similar materials and can be considered as typical for the ply [5]. The engineering constants for the laminate were determined using laminate analysis software and entered to the element material properties.

Table 1. Ply properties used in the analyses.

Property	Value
E_1	54 GPa
E_2	54 GPa
G_{12}	4.5 GPa
ν	0.03
σ_{1t}	540 MPa
σ_{1c}	380 MPa
σ_{2t}	540 MPa
σ_{2c}	380 MPa
τ_{12}	90 MPa

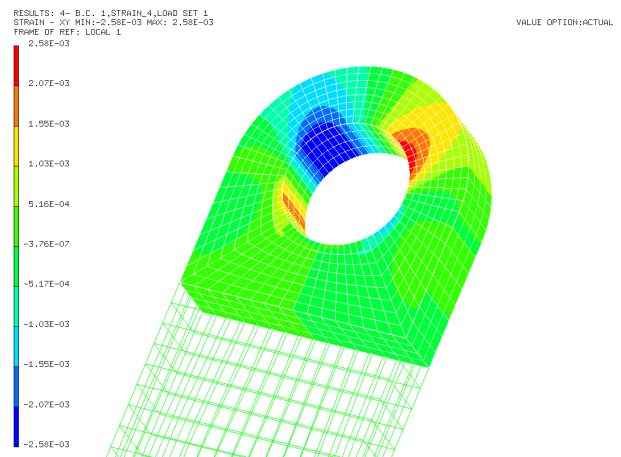


Fig. 5. In-plane shear strains in straight tension, $F = 100$ kN.

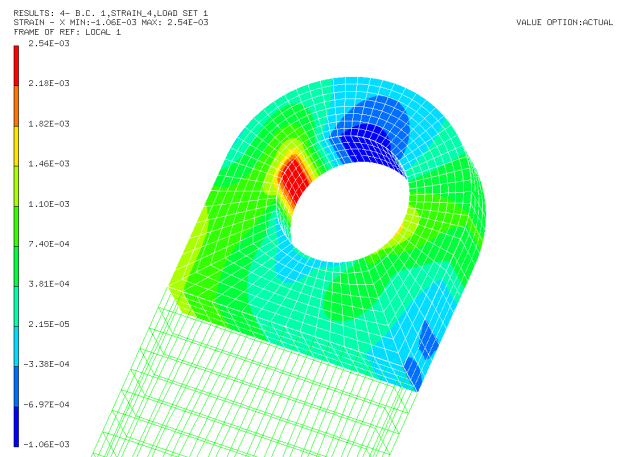


Fig. 6. Normal strains in 27° angle tension, $F = 100$ kN.

3.3 Analysis Results

The results of the FE-analyses are presented in Figs. 4-7. The load in the contour plots corresponds to the 100 kN loading in the test. The failure loads in both load cases were estimated assuming two different failure modes: tensile failure and shear failure. The analysis was therefore performed in two separate locations corresponding to the maximum normal strain and maximum shear strain.

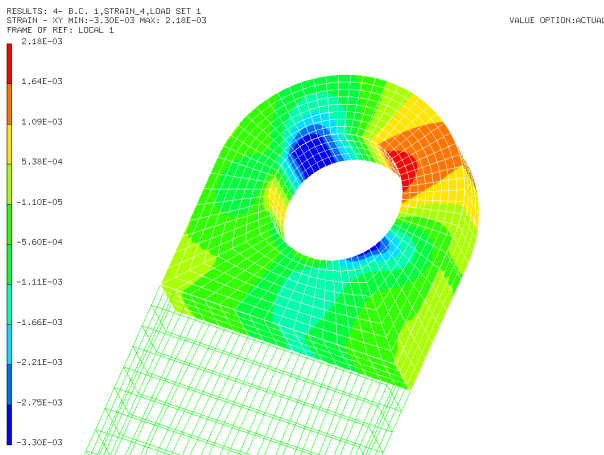


Fig. 7. In-plane shear strains in 27° angle tension, $F = 100$ kN.

3.4 Test Prediction

The expected failure loads according to the analyses are presented in Table 2.

The strain values used in failure analyses are nodal values around the hole, i.e. characteristic distance was not applied. The minimum size of the element around the hole was 4.4 mm. The use of nodal values around the hole was considered to result in conservative failure load estimation.

The strain values were applied to laminate analysis software and the failure loads were computed with the Tsai-Hill criterion.

In straight tension the estimated failure mode was a tensile failure. The shear failure load was only 4.4% higher. In 27° angle tension the failure mode was estimated to be a shear failure. The tensile failure load was 19% higher.

Table 2. Estimated failure loads.

	Straight tension		27° angle tension	
	Failure load [kN]	Critical ply	Failure load [kN]	Critical ply
Max σ	383	0/90	338	0/90
Max τ	400	±45	283	±45

4 Testing

The purpose of the test was to prove feasibility of the chosen lug geometry, to find out load carrying capability of the undamaged lug and to validate the FE-analyses. Five specimens were tested.

4.1 Test Specimens

The test specimens were manufactured with the RTM technique. A flat mold was used to inject a solid CFRP block (360×150×39.2 mm). The final shape of the lug, including the attachment holes for the test fixture, was machined. The sliding bearing was installed using interference fit. Adhesives were not used.

All specimens were ultrasonic scanned after manufacture. Four of them showed significant attenuation in the C-scan. Visual inspection revealed that most of the porosity was located near the surface of the lug, see Fig. 8. Therefore, it was decided not to discard the specimens but to use them as originally planned.

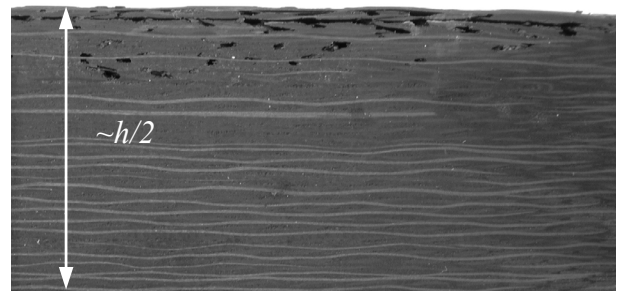


Fig 8. Porosity near the surface of the test specimen.

The dimensions of one lug were smaller than in other specimens due to an error in machining. The specimen was included in the test matrix as a separate item. The width of the specimen was 136 mm.

The test matrix is presented in Table 3.

Table 3. Test matrix.

Loading	Number of specimens	Instrumented specimens
Straight tension	2	1
27° angle tension	2	1
Small specimen	1	1 ¹

¹Reduced number of strain gages.

4.2 Test Arrangement

4.2.1 Test Fixture

Steel plates were attached on both sides of the lug using four fasteners (double lap joint). The thickness of the plates was 25 mm and fasteners were M16 steel bolts. In the 27° angle tension the specimen is rotated by steel plates that form

a 153° angle with the lug. The other end of the joint was connected to the loop end of the hydraulic actuator. The load to the lug was applied using a fork end and a steel pin (Ø70 mm). The test arrangement is illustrated in Fig. 9.

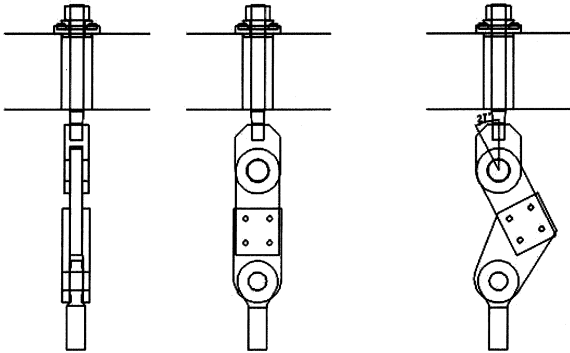


Fig 9. Schematic view of the test arrangement.

During the tests the test fixture had to be modified because the maximum load capacity of the hydraulic actuator was reached without specimen failure in both straight tension and 27° angle tension. The maximum applied load was 437 kN, i.e. well above the predicted failure loads in both load cases.

The new fixture was in principle similar to the previous one. The size of the test fixture attachment bolts was increased to M22 and the holes in the specimen had to be expanded accordingly.

The increased risk of having a premature failure in the specimen along the bolts was recognized. Therefore, the bolt holes were moved towards the centerline of the specimen. Thus, the distance from the hole edge to the specimen edge was not reduced.

4.2.2 Specimen Instrumentation

Two of the specimens were equipped with 6 strain gages. Five strain gages were positioned according to Fig. 10 and the sixth strain gage was positioned to measure through-the-thickness strain. The numbers 3 and 4 denote same position on opposite sides of the lug. The small specimen was equipped with two strain gages measuring the normal strain in the critical

location on both sides of the lug (positions 1 and 2).

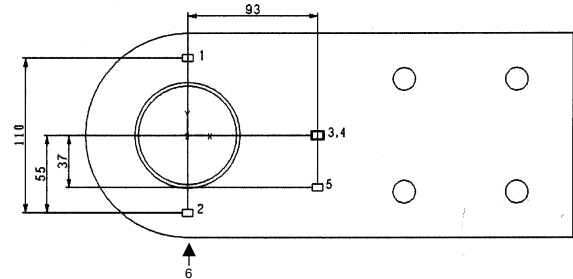


Fig 10. Positions and numbering of the strain gages.

4.3 Lug Tests

The lug tests were done in two phases because the maximum load of the hydraulic actuator was reached. New test fixture was designed and this caused some differences in the measurements between test phases.

4.3.1 Load Response of the Lug

The load response results were obtained with the first test fixture. Four specimens were tested, three in straight tension and one in 27° angle tension. One of the straight tension test specimens was the small specimen. None of the specimens reached the failure load.

The first specimen tested in straight tension was used to verify overall reliability of the test arrangement and had no strain gages. The specimen was tested up to 434 kN.

The second specimen was also tested in straight tension. This specimen was equipped with six strain gages. It was loaded up to 437 kN. The results are presented in Fig. 11. It can be seen that the specimen behavior is linear and residual strains are small. The strains from gages 1 and 2 are almost identical. However, strain gages 3 and 4 produce different results indicating bending on the specimen.

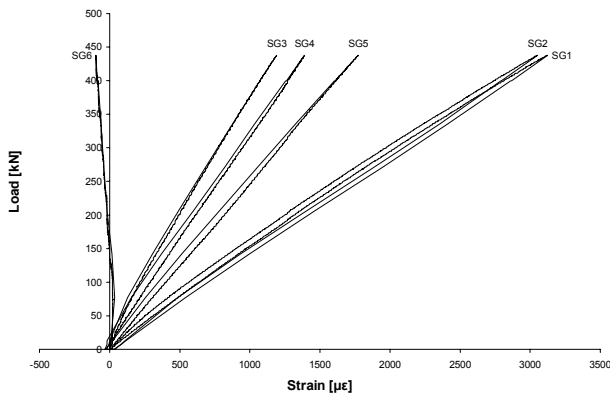


Fig 11. Load response of the straight tension specimen.

The third specimen equipped with six strain gages was tested in 27° angle tension. The specimen was also tested up to 437 kN without failure. The measured strains are presented in Fig. 12. The behavior is similar to the behavior of previous specimen.

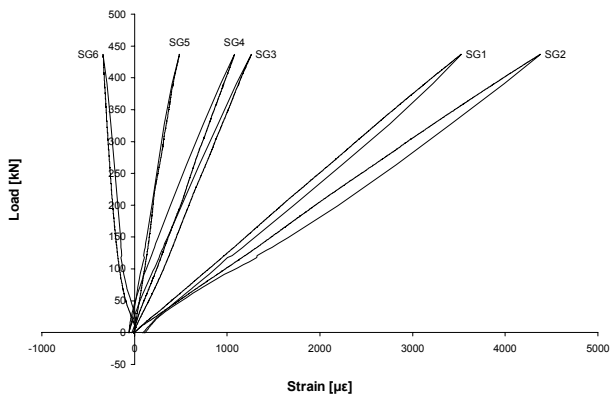


Fig 12. Load response of the 27° angle tension specimen.

The small fourth specimen was tested in straight tension and had two strain gages. Also in this case the maximum force of the hydraulic actuator was achieved without failure. The results of the two strain gages are presented in Fig. 13. Again the behavior is linear and strains are close to each other.

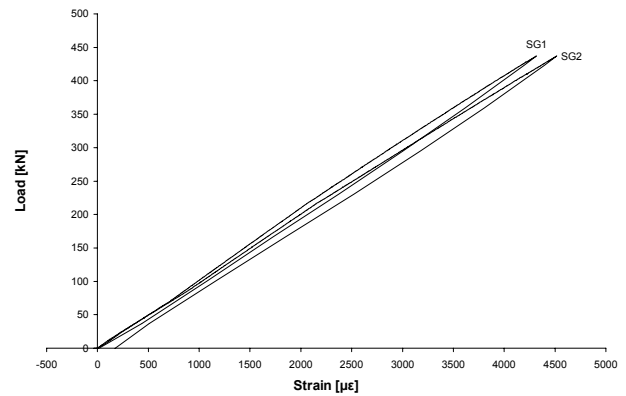


Fig 13. Load response of the small specimen in straight tension.

Because the failure load could not be reached using this test arrangement the last specimen in the test matrix was not tested before the new test fixture was available.

4.3.2 Failure of the Lug

With the new test arrangement the failure loads of the lugs were possible to achieve. A summary of the results are presented in Table 4.

Table 4. Failure loads of specimens.

Specimen	Straight	27° angle	Failure load [kN]	Note
1	×		596	
2	×		598	
3		×	474	Failure in bolt level
4	×		539	Smaller specimen
5	×		576	Load direction changed ¹

¹Originally planned to be tested in 27° angle tension.

The first specimen was tested in straight tension without strain gages. Therefore, only failure load is available. The failure occurred in the critical location as predicted by the analysis. The failure mode was tensile failure as shown in Fig. 14.

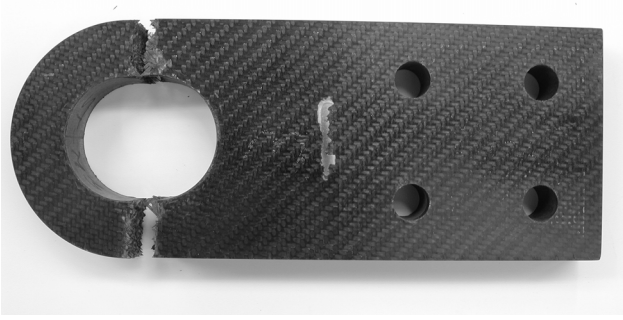


Fig 14. Typical failure mode of the straight tension test specimen.

The second specimen was tested in straight tension. Measured strains are presented in Fig. 15. The behavior of the specimen was linear up to failure. The strains 1 and 2 are even closer to each other than in the previous testing. The same applies to strains 3 and 4 showing less bending in the specimen than in the first set of tests.

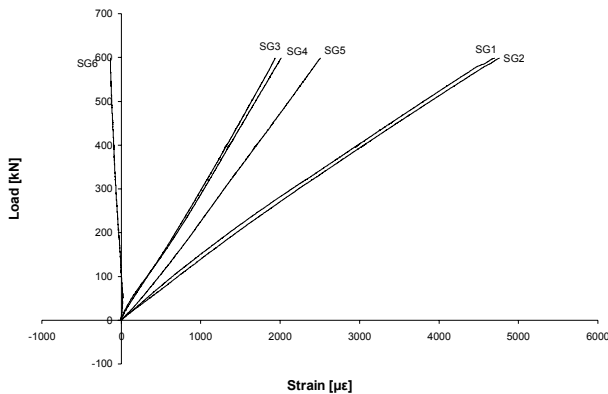


Fig 15. Failure of the straight tension specimen.

Strains of the third specimen are presented in Fig. 16. The specimen was tested in 27° angle tension. Some nonlinearity can be seen but the overall behavior is quite linear. The strain results from the first and second tests are not fully comparable because the direction of the loading was changed, i.e. the specimen was rotated in the test fixture.

The test was not fully successful because the specimen failed along the attachment points (see Fig. 17). Thus the failure load could not be determined. As a consequence the other specimen planned to be tested in 27° angle tension was finally tested in straight tension.

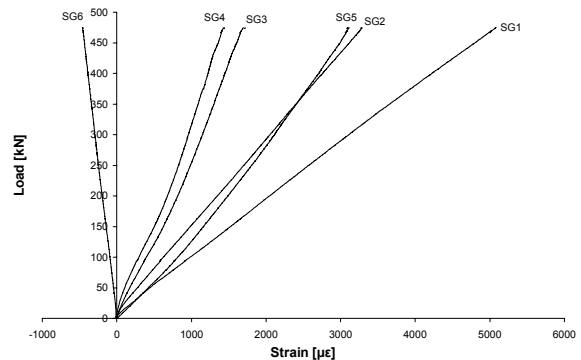


Fig 16. Failure of the 27° angle tension specimen.

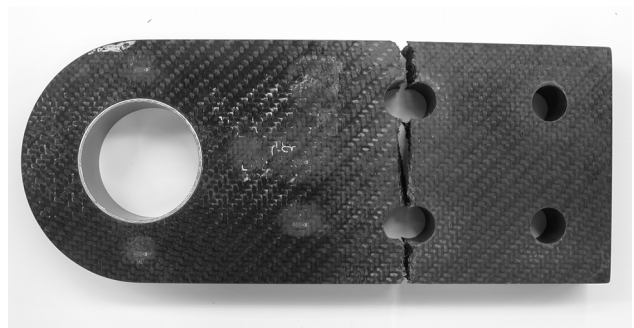


Fig 17. Failure of the 27° angle tension specimen.

The strains of the fourth specimen (small specimen with two strain gages) are presented in Fig. 18. The behavior is similar to the behavior of the other specimens.

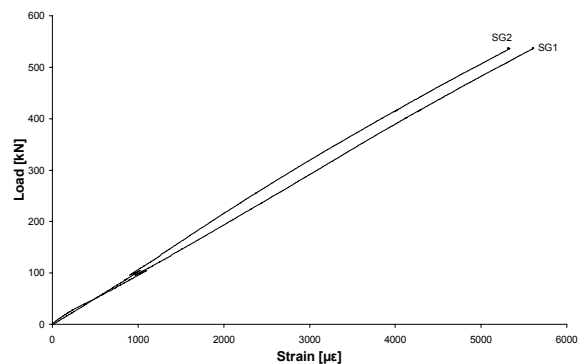


Fig 18. Failure of the small specimen in straight tension.

The fifth specimen was planned to be tested in 27° angle tension but was finally tested in straight tension. The specimen had no strain gages. Only the failure load was measured.

4.4 Laminate Tests

Laminate level tests were performed with the sublaminates 1 used in the lug structure. Standard tensile tests were made to determine the modulus and strength of the laminate. The results are presented in Table 5. The specimen was a straight coupon with tabs bonded on both ends. The dimensions of the specimen were 200×20×6 mm. The number of specimen was 10.

Table 5. Results of the laminate level tests.

Specimen	E_x [GPa]	σ_x [MPa]
Average	34.30	393.5
Deviation %	2.08	2.3

5 Test Analyses

The estimated strains in straight tension test are compared with the measured ones in Table 6 and in 27° angle tension in Table 7. The measured values are obtained from the load level 430 kN and the analysis results are scaled up accordingly.

Table 6. Measured and estimated strains in the straight tension specimen. Measurements are based on the second specimen tested up to failure (Fig. 15).

Strain gage	Measured [%]	Estimated [%]	Difference [%]
1	0.323	0.340	+5
2	0.331	0.340	+3
3	0.143	0.129	-10
4	0.146	0.129	-12
5	0.183	0.194	+6
6	-0.010	-0.054	+4

Table 7. Measured and estimated strains in the 27° degree tension specimen. Measurements are based on the third specimen tested up to failure (Fig. 16).

Strain gage	Measured [%]	Estimated [%]	Difference [%]
1	0.457	0.367	-20
2	0.298	0.318	+7
3	0.154	0.133	-14
4	0.129	0.133	+3
5	0.287	0.323	+13
6	-0.042	-0.069	+64

The correspondence can be considered good in the straight tension tests, because the material properties were based on estimated

values. In 27° angle tension tests significant differences exist between the measured values and the predicted ones. Higher strain gradients in the 27° angle tension combined with small positioning errors of the strain gages and the specimen are the probable reason for the deviation.

The estimated failure loads in both load cases are compared to the measured ones in Table 8. The estimated failure load for the small specimen is obtained using a scale factor. The scale factor used was defined as the ratio between the reduced and original width of the specimen resulting to 0.934. The measured scale factor is defined as the ratio between the failure load of the small specimen and the average failure load of other straight tension test specimens.

Table 8. Measured and estimated failure loads.

Straight tension	Measured [kN]	Estimated [kN]	Difference [%]
Average	590	383	-35
Small spec.	539	359	-33
Scale factor	0.914	0.934	+2

Table 8 points out that the failure loads were significantly underestimated. The estimated scale factor corresponds well with the measured one. However, it should be noted that only one test result for the small specimen was available.

Stiffness and tensile strength values estimated for the sublaminates 1 with ply properties in Table 1 are compared to the measured ones in Table 9.

It can be seen that the differences between measured and estimated values are similar as in the lug tests. Thus, analysis results with correct ply properties would match fairly well with the measured ones.

Table 9. Measured and estimated results of the laminate level tests.

Laminate 1	Measured	Estimated	Difference [%]
E_x [GPa]	34.3	33.03	-4
σ_x [MPa]	393.5	258	-34

6 Conclusions

According to the results obtained the following conclusions can be made:

The composite lug manufactured from a solid laminate and machined to shape seems to be a feasible solution even with the small edge distance that was used in the tests. However, more testing is needed e.g. to study damaged specimen behavior, the effect of environmental exposure and fatigue of the lug.

The engineering type FE-approach as an analysis method can provide a reasonable estimate on the behavior of the lug.

The ply properties used in the analyses did not completely correlate with the test results of the sublaminates 1. Especially the strength values were considerably underestimated.

The failure load of the lug is possible to estimate with sufficient accuracy if correct material values are available.

The specimen behavior was linear up to the failure load of the lug.

Acknowledgements

The research described in this paper was carried out at Helsinki University of Technology, Laboratory of Lightweight Structures under a contract and co-operation with Patria Finavicomp.

References

- [1] Niu M. C. Y. *Airframe structural design*, 1st edition, Conmilt Press Ltd. 1989, 612 p.
- [2] Koljonen J, Pentto F, Wallin M. *Tension tests for composite hinge lugs*. Test plan and report (restricted) 2002, 22 p.
- [3] I-DEAS Master series 8, EDS-PLM Solutions.
- [4] ESAComp version 2.0, Compoengineering Inc.
- [5] Viitanen T. *Screening of thermosets for high-temperature polymer matrix composites*. Master's thesis. Helsinki university of technology 1999. 171 p. (in Finnish).